ON THE ORIGIN OF JOVIAN DECAMETER RADIO BURSTS

P. Zarka*, B. P. Ryabov†, V. B. Ryabov†, R. Prangé‡,
M. Abada-Simon§, T. Farges§, and L. Denis¶

Abstract

Jovian "millisecond"or "S" bursts are intense impulsive decameter radio spikes, drifting in frequency in tens of milliseconds over several MHz, which generation scenario has been much debated for 30 years. The result of automated recognition and analysis applied to an extensive set of ground-based digital high-resolution observations of these bursts strongly favours an emission mechanism and scenario: Cyclotron-Maser emission of electron populations accelerated near Io, and then in quasi-adiabatic motion along magnetic field lines connecting Io's magnetospheric wake to Jupiter's auroral regions. In this frame, the energy and pitch angle of radiating electrons, the location of the field lines along which they emit radio waves with respect to Io's flux tube, and the radiosources extent are deduced from radio measurements. However, when compared to the results of Voyager in-situ exploration of Io's vicinity, and to recent InfraRed and Far-UltraViolet observations of the Io flux tube footprint, the Cyclotron-Maser mechanism meets an "energy crisis". On another hand, the very fine frequency-time structure of S-bursts displays complex patterns, here interpreted as the signature of small-scale and short-lived density and/or acceleration structures, while their average properties are attributed to the magnetic field topology near the IFT and the sharp emission beaming.

1 Introduction

About 10% of Jupiter's decameter radio emission is detected under the form of very short and intense bursts drifting in the frequency-time plane (Figure 1a). First observed shortly after the discovery of Jupiter's decameter emission [Gallet, 1961], they have been called S-bursts (where "S" stands for "Short") in reference to their sporadicity at the millisecond timescale, by contrast with the more usual Jovian emissions which exhibit variations at the minute-to-hour timescale and have been -not so properly- qualified "L" (for Long) bursts.

*DESPA, CNRS/Observatoire de Paris, F-92195 Meudon, FRANCE
†Institute of Radioastronomy, Krasnoznamennaya 4, Kharkov 310002, UKRAINE
‡CNRS/Institut d'Astrophysique Spatiale, F-91405 Orsay, FRANCE
§ARPEGES, CNRS/Observatoire de Paris, F-92195 Meudon, FRANCE
¶Station de RadioAstronomie de Nançay, USR B704, Observatoire de Paris, 18 Nançay, FRANCE

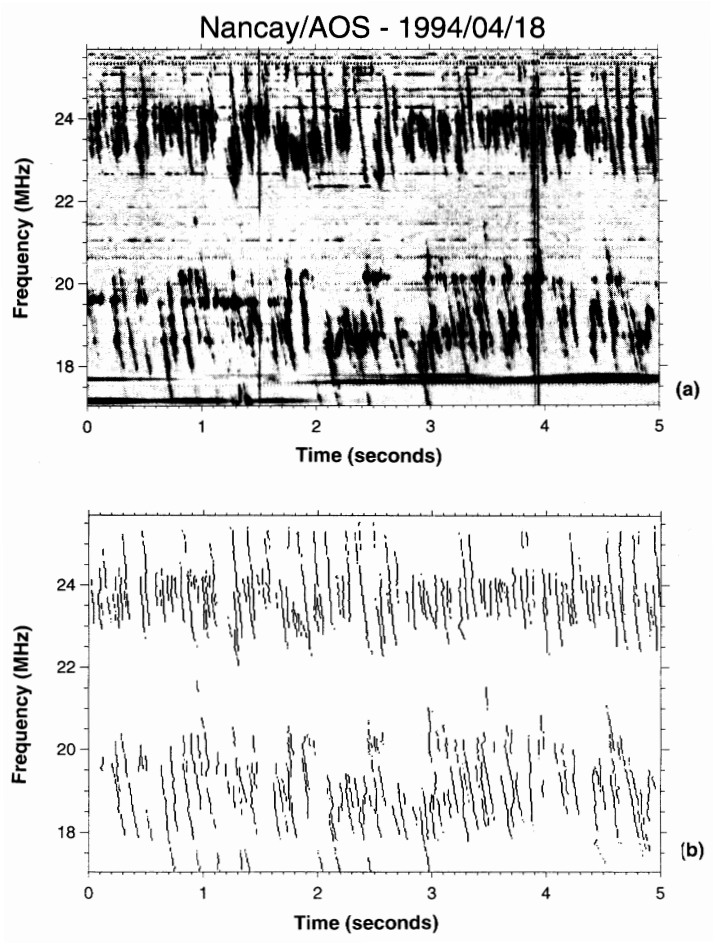

Figure 1: (a) Dynamic spectrum of Jovian S-bursts recorded during a radio storm on 1994/04/18 with the Nançay Acousto-Optical Spectrograph. This spectrograph operates as a multichannel receiver, sampling simultaneously for 10 msec 2048 channels covering a total band of 26 MHz. Darkness is proportional to intensity. Negative drift-rates are obvious at this time resolution of 10 msec. (b) Result of automated S-bursts recognition. Based on the "images" (a) and (b), physical characteristics of the emission (bandwidth, duration and drift-rate) are measured on a regular frequency grid with 200 kHz spacing.

S-bursts are much more than an "exotic" component of Jupiter's radio spectrum. Their study connects to broader questions :

- They might be a prototype for planetary radio bursts, which have been detected at all the giant "radio-planets" (Saturn, Uranus, Neptune - see Kaiser et al., [1984]; Desch et al., [1991]; Zarka et al., [1995]) in the kilometer range by Voyager's Planetary Radio Astronomy experiment with a low time resolution (6 sec.) swept-frequency receiver; also the Earth's auroral kilometric radiation dynamic spectra are almost exclusively made of narrowband fast drifting features (see Zarka, [1992], and references therein). However, only Jovian S-bursts reach decameter wavelengths and are thus detectable from the ground - above the Earth's ionospheric cutoff at $5 - 10$ MHz -, from where they can be extensively studied with high frequency and time resolutions spectrographs [Riihimaa, 1991].

- At Jupiter, radio bursts are strongly "controlled" by the satellite Io, i.e. they are detected only in two particular configurations of the Io-Jupiter-observer angle (see section 2 below); this implies that the source location is directly linked to Io's position. The role of Io may imply a crucial difference in the nature of Jovian S-bursts as compared to the other planetary radio bursts, but alternatively Io may just represent a particular source of electron acceleration to be compared to other sources (tail magnetic field reconnection, magnetopause surface waves, etc.) in the other planetary magnetospheres. In any case, the S-bursts source region is much better known than any other planetary low-frequency radiosource, and the increasingly better knowledge of the magnetic field topology [Connerney et al., 1996] and plasma population [Divine and Garrett, 1983; Meyer-Vernet and Moncuquet, this volume, and references therein] in its vicinity allows for serious modelling of S-bursts generation. Conversely, the rich morphology of S-bursts dynamic spectra makes them a good "tracer" of the Io-Jupiter electrodynamical circuit, and may reveal small-scale acceleration regions in the vicinity of Io's Flux Tube (see section 5 below).
- Observations of the Io Flux Tube (IFT) footprint in the IR and UV ranges have begun to appear [Connerney et al., 1993; Prangé et al., 1996]. They are very complementary to the decameter ones, especially in terms of spatial resolution. Comparison of the observations in the 3 frequency domains allows to draw an energy budget of the Io-Jupiter electrodynamical interaction, which raises new questions (see section 6 below).
- Understanding the Io-Jupiter interaction may lead to a generalization to other pairs of magneto- ionized interacting bodies (for example magnetized binary stars).
- Finally, Jovian S-bursts are the most powerful radio emission in the solar system : with a flux density up to 10^{-16} W m^{-2} Hz^{-1} at 1 A.U. distance, they compete with the most powerful solar type III bursts. The direct search of Jovian-like radio bursts at decameter wavelengths is thus a promising way in the recent field of exoplanet search (already in progress - see Zarka et al., [this volume]).

2 Summary of S-Bursts Properties

Since their discovery in 1961 [Gallet, 1961], over 40 papers have dealt with S-bursts observations and derivation of characteristic properties (see for example Leblanc et al., [1980b]; Ellis, [1982]; Dulk et al., [1992]; Zarka et al., [1996] and references therein). Among them, less than 10 have been published since 1984, mainly due to limitations of the instrumentation which did not allow until recently to perform the necessary digital observations with high frequency and time resolutions (see section 3 below).

At the time of the "Planetary Radio Emissions III" meeting (1991), the S-burst physical properties could be summarized as follows :

- As written above, they represent $\sim 10\%$ of the total Jovian decameter radio emission occurrence probability, and they are detected only when the Io-Jupiter-observer

angle (as viewed from the north of the ecliptic plane) is $+90° \pm 10°$ (so-called "Io-B source", corresponding to Io about 6h Local Time for an observer on the Earth) and $-50° \pm 10°$ ("Io-A source", with Io about 15h20m Local Time) [Riihimaa, 1977; Ellis, 1982; Alexander and Desch, 1984; Genova and Calvert, 1988].

- The dominant S-bursts polarization is right-handed circular or elliptical, which corresponds to the extraordinary magneto-ionic mode in Jupiter's northern hemisphere.
- The brightness temperature is extremely high ($\geq 10^{17}$ K), indicating a non-thermal coherent generation process, and corresponds to an instantaneous power over $10^8 - 10^9$ W during a burst.
- Instantaneous bandwidth is a few kHz, and duration at fixed frequency is a few milliseconds; in the frame of electrons moving along magnetic field lines in Io's vicinity (L-shell ≈ 6) and generating radio emission at the local gyrofrequency, these values convert to an instantaneous parallel source size smaller than ~ 20 km. The typical overall bandwidth and duration of a burst are 0.5 to 2 MHz and 50 to 100 msec, corresponding to an overall parallel source size about $1000 - 2000$ km.
- Finally, the most remarkable characteristic of S-bursts is their rapid drift in the f-t plane, generally negative (i.e. from high to low frequencies), over several MHz at a variable rate about tens of MHz/s (Figure 1). The absolute value of the drift-rate has been found to increase roughly proportionally to the frequency, up to ~ 30 MHz (open dots on Figure 2).

The microscopic generation mechanism for S-bursts is generally assumed to be the same as for the L-bursts or the other planetary auroral radio emissions, i.e. Cyclotron-Maser emission from unstable populations of energetic electrons, but the macroscopic "scenario" in the frame of which this mechanism operates is certainly specific to the S-bursts and linked to the Io-Jupiter circuit.

3 Drift-Rates in the Frequency-Time Plane

Drift-rates are the most constraining characteristic for building a scenario for S-bursts generation. If the instantaneous emission occurs near the local electron cyclotron frequency, negative drifts suggest that the radiating region moves upwards during a burst, i.e. away from the planet. As the motion of Io (and its conductive ionosphere) through Jupiter's magnetic field is expected to dissipate energy, in particular under the form of electron acceleration, an "adiabatic" emission scenario was proposed [Ellis, 1965; Goldreich and Lynden-Bell, 1969; Kawamura and Suzuki, 1976; Krausche et al., 1976] in which electron bunches are accelerated near Io and precipitate along Jovian field lines. The conservation of their first adiabatic invariant and total energy slows their parallel motion down to their mirror points where they are reflected back. Electrons with larger $v_\parallel / v_\perp$ have a lower mirror point and can thus be lost through collisions in the upper ionosphere, so that the reflected population is expected to possess a "loss-cone" feature susceptible to amplify cyclotron radio waves [Wu and Lee, 1979].

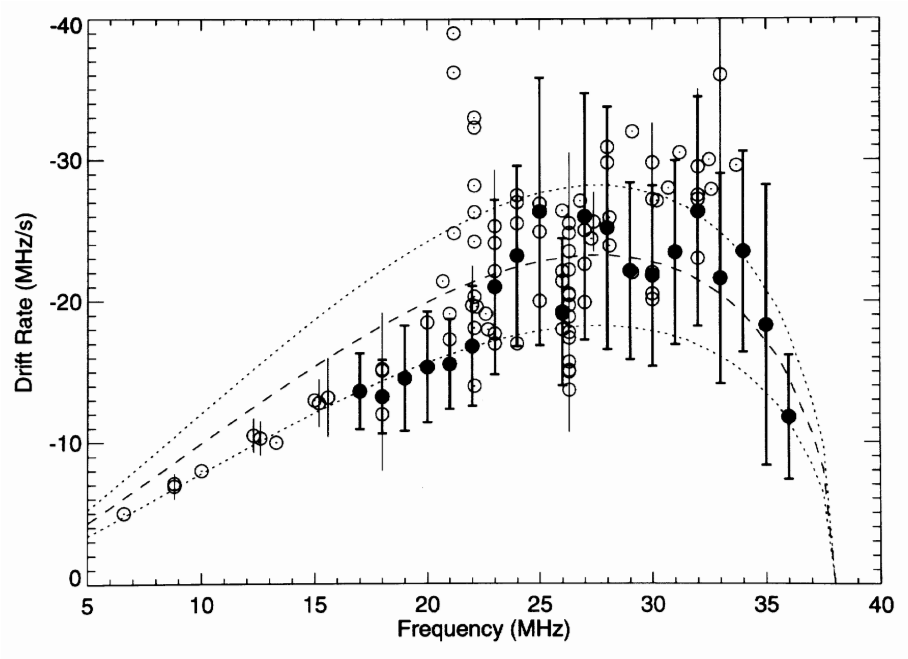

Figure 2: S-bursts drift rates versus frequency. Previous results (1965 to 1991, concerning mainly the Io-B source) are summarized by open dots . Our results (solid dots) are consistent with previous ones but reach higher frequencies and are based on a much larger number of measurements (500 to 6000 at any frequency between 17 and 33 MHz, 422 at 34 MHz, 114 at 35 MHz and 8 at 36 MHz). Each solid dot and associated vertical bar are the peak of the drift-rates distribution at the corresponding frequency and its dispersion (± 3 to ± 8 MHz/s) due to intrinsic drift-rates variations within a storm or from one storm to the other. The theoretical curves are computed from the adiabatic scenario (Eq. 1) with $\Phi_e = 2.8°$ and $v = 0.14c$ (dashed line) $\pm 0.03c$ (dotted lines). Changing Φ_e by $0.1°$ would shift the curves laterally by $2-3$ MHz.

In a dipolar field, the drift-rate df/dt of S-bursts produced by such "quasi-trapped" electrons can be formulated analytically:

$$\begin{aligned} df/dt &= -3/(L \cdot R_J) \cdot g(\Theta) \cdot f \cdot v \cdot [1 - \sin^2(\Phi_e) \cdot 2\pi m_e \cdot f \cdot L^3/(B_e \cdot e)]^{1/2} \\ &\approx -K \cdot f \cdot v_{\parallel}(f) \end{aligned} \qquad (1)$$

L being the distance in Jovian radii ($1R_J = 71400$ km) at which the field line intersects the magnetic equator, and Θ the magnetic colatitude. $g(\Theta) = (\cos\Theta/\sin^2\Theta) \cdot (3 + 5\cos^2\Theta)/(1+3\cos^2\Theta)^{3/2}$ is nearly constant in the auroral regions, $v = |\mathbf{v}|$, Φ_e is the equatorial pitch ($\mathbf{v} - \mathbf{B}$) angle, and B_e the equatorial magnetic field at $1R_J$ (see Zarka et al., [1996]). As $K \approx$ constant and $v_{\parallel}(f)$ decreases with increasing frequency f, the acceleration of the upgoing electrons (adiabatic increase of $v_{\parallel}$) competes with the $\sim 1/r^3$ decrease of the gyrofrequency so that $|df/dt|$ is expected to reach a maximum for $20 < f < 30$ MHz (depending on the magnetic dipole moment used).

Most of the drift-rates measurements performed for Io-B emission until 1991 are reported on Figure 2 (open dots, all below 33.7 MHz - see Zarka et al., [1996] and references therein). They failed to confirm the decrease of $|df/dt(f)|$ at high frequencies expected

from the adiabatic scenario, so that alternative theories were proposed for S-bursts generation, from the addition of ad-hoc parallel electric fields accelerating upgoing pulsed electron beams just above Jupiter's ionosphere [Desch et al., 1978; Flagg and Desch, 1979; Leblanc et al., 1980b; Ellis, 1980; Melrose, 1986] to more intricate processes including for example waves conversion or beating [Zaitsev et al., 1986; Boev and Luk'yanov, 1991a], magneto-drift radiation of MeV electron beams [Ryabov, 1994] or radio lasing in a size-variable cavity [Calvert et al., 1988]. However, S-bursts occurrence is scarce at high frequencies, and the increasing dispersion of $|df/dt|$ with f visible on Figure 2 is an intrinsic characteristic of S-bursts, and not due to measurement errors. A large number of homogeneous measurements was thus needed to constrain and test the proposed models.

Those have been performed through the automated recognition and analysis (Figure 1b) of several thousands of S-bursts digitally recorded with an Acousto-Optical spectrograph connected to the decameter arrays of Nançay (France, [Boischot et al., 1980b]) and Kharkov (Ukraine, [Braude et al., 1978]), with resolutions of $\delta t = 10$ msec per spectrum and $\delta f = 13$ kHz over a 26 MHz total band. The results, also displayed on Figure 2 (solid dots and dispersion bars), reveal a decrease of $|df/dt|$ at high frequencies, supporting the adiabatic scenario for S-bursts generation [Zarka et al., 1996].

A fit with Eq. (1), using a dipolar field model with $B_e = 7$ Gauss (allowing for gyrofrequencies > 36 MHz along the $L \approx 6$ field line), gives electron velocities of $v = 0.14c \pm 0.03c$ and pitch angle $\Phi_e = 2.8° \pm 0.1°$. The corresponding characteristic energy of the radiating electron population, measured for the first time, is $E = 5.3 \pm 2.2$ keV, very similar to that measured in the terrestrial kilometric radiation sources [Hilgers and de Feraudy, 1992]. The source altitude extends from $\sim 0.01 R_J$ at 36 MHz to $\sim 0.28 R_J$ at 17 MHz (Figure 3a). The average parallel electron velocity in the source is $v_{\|} = 22000 \pm 2000$ km/s. The observed S-bursts total bandwidth ($\triangle f = 0.5 - 3$ MHz) and duration ($\triangle t = 50 - 100$ msec) imply an overall wave-particle interaction region $\triangle r \approx 1000 - 2500$ km for each burst, while the instantaneous bandwidth (≤ 20 kHz) and duration (< 10 msec) correspond to an instantaneous source extent $\delta r \leq 20$ km, in agreement with previous works.

Although confirming the relevance of the adiabatic scenario for the generation of S-bursts by quasi- trapped electrons, the large intrinsic dispersion of the measured drift-rates does not exclude the existence (possibly non-permanent) of upwards accelerating electric fields above the auroral ionosphere. The deduced parallel speed ($\sim 2 \times 10^4$ km/s) might be that of an instability threshold moving along magnetic field lines (i.e. a phase velocity) rather than the actual velocity of electron populations. In support of a Cyclotron-Maser type microscopic emission mechanism, one can note that the total frequency range of the S-burst emission (~ 17 to 25.5 MHz in Figure 1, and 17 to 36 MHz in all our measurements of Figure 2) approximately matches along the source field lines a region between the mirror points of the reflected electron population and the altitude where, due to the adiabatic motion, the electrons perpendicular energy no more dominates the parallel one (i.e. where $E_{\perp} \approx E_{\|}$). At this stage, Cyclotron-Maser emission is quenched by the disappearance of strong perpendicular velocity gradients in the electronic distribution function ($\partial f/\partial v_{\perp}$).

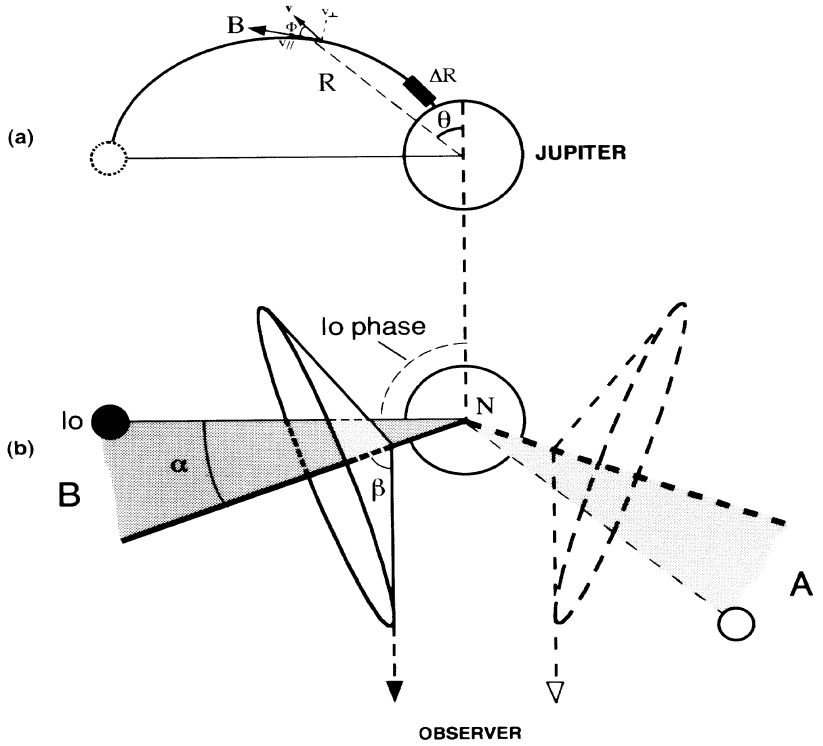

Figure 3: (a) Geometry of the Io ($L = 6$) field line. S-burst emission between 17 and 36 MHz takes place along its boldface part. The quantities used in the calculations (v, $v_\perp$, $v_\parallel$, Φ, $\triangle R$) are indicated. (b) Sketch of the Io-Jupiter interaction presented in our scenario, in projection onto the equatorial plane. A and B label the geometries of the corresponding decameter radio "sources". The Io phase is counted from the anti-observer's direction. The case for a phase of 90° ("B" source), studied here, is emphasized. Due to the rapid magnetospheric corotation (in ~ 10 hours), its wake (shaded) precedes Io in its orbital motion. The boldface line represents the "active" field line along which most of the S-burst emission is inferred to occur, after electron acceleration by Alfvèn waves in Io's wake. The radio emission is beamed at large angle from the source magnetic field, along the walls of a cone of aperture β. The values of α and β are derived in the text. The real situation is more complex than sketched (magnetic field lines are not included in a meridian plane).

4 IR & UV Observations, Emission Scenario and Energy Crisis?

Several authors attribute electron acceleration by Io to the Alfvèn waves trains (so-called "Alfvèn wings") -generated by Io's perpendicular motion through the Jovian magnetic field-, which have been discovered by the Voyager spacecraft in Io's magnetospheric wake [Acuña et al., 1981; Belcher et al., 1981; Gurnett and Goertz, 1981; Goldstein and Goertz, 1983]. In a reference frame fixed with respect to the IFT, these waves possess parallel electric fields susceptible to accelerate electrons. This process is not instantaneous, and a lag (α) is expected between the instantaneous Io field line and the "active one", along which radio waves are produced. Assuming a constant α, considerations of symmetry between Io-A and Io-B sources immediately imply $\alpha \approx 20°$ and a radio emission beaming angle $\beta \approx 70°$ with respect to **B** in the source (as sketched on Figure 3b). Actually, taking into account the 3-D geometry and a magnetic field model more realistic than a

Table 1: Characteristics of near-IFT emissions in the UV, IR and Radio ranges and comparison to Alfvèn waves properties.

	FUV[a] (H_2)	IR[b] (H_3^+)	Radio/decameter[c] (S-burst)	Alfvèn waves[d]
Occurrence	?	weak surface $\|\mathbf{B}\|$	strong surface $\|\mathbf{B}\|$	downstream "wings"
Lag w.r.t. instantaneous IFT footprint (O6)	variable ($1° - 10°$ N, $4° - 12°$ S)	variable ($15° - 20°$)	variable ($10° - 20°$)	a few (2?) degrees
Energy of precipitations (e^-, p^+)	e^-: $1 - 200$ keV p^+: $25 - 500$ keV	?	e^-: 5 ± 2 keV	e^-: $1 - 500$ keV $< E >= 78$ keV
Observed or computed emitted power	$5 \cdot 10^{10}$ W	$3 - 10 \cdot 10^{10}$ W	10^8 to $\geq 10^9$ W	a few 10^{11} W (total) a few 10^9 W (keV range)
Deduced incident (precipitated) power	$2 - 3 \cdot 10^{11}$ W	a few 10^{11} W	10^{10} to $\geq 10^{11}$ W (perpendicular energy of keV e^-)	$\sim 2 \cdot 10^{12}$ W per hemisphere

[a] Prangé et al. [1996]
[b] Connerney et al. [1993]
[c] Zarka et al. [1996]
[d] Crary [1997] and references therein

dipole (O6 model, [Connerney, 1992; Connerney et al., 1996]), one finds $\alpha \approx 10° - 25°$ and $\beta \approx 70° - 80°$. These values of β are perfectly consistent with our present knowledge of planetary radio emission beaming [Zarka, 1988]. The Alfvèn wings model provides a possible explanation for the "multiple- arc" structure found in radio emissions dynamic spectra from Voyager and ground-based observations [Gurnett and Goertz, 1981; Carr et al., 1983]. Finally, one should note that S-bursts occurrence is higher when the IFT footprint sweeps through region of high field magnitude on the planetary surface [Genova and Calvert, 1988; Aubier et al., 1988].

Recent IR and FUV observations of the IFT footprint are now available, which can compare to the above results and allow to perform an energy budget of the precipitations in the vicinity of the IFT [Connerney et al., 1993; Prangé et al., 1996]. They are summarized in Table 1, together with the relevant Radio results. The observed lag between the IR (resp. UV) spot and the instantaneous Io field line (O6 model) is variable, typically between 15° and 20° (1°-12° in UV). An isolated spot is observed (slightly elongated in IR), inconsistent with the multiple-arc patterns observed in radio dynamic spectra. The radiated power is $\sim 5 \cdot 10^{10}$ W in UV (H_2 bands) and $3 - 10 \cdot 10^{10}$ W in IR (Joule heating) from which one deduces a power input from the precipitations of a few 10^{11} W, consistenly in the IR and UV ranges. This Figure seems also consistent with the $10^8 - 10^9$ W radio output, taking into account the maximum efficiency of the Cyclotron-Maser mechanism $< 1\%$. It represents a large fraction ($\sim 1/4$) of the total system energy provided by Io's motion across Jovian magnetic field lines, estimated as of

the order of 10^{12} W per hemisphere ($\approx 2 \cdot R_{Io} \cdot E \cdot I$, with the electric field E across Io being $E \approx v \times B \approx 6 \cdot R_J \cdot \Omega_J \cdot B_e/6^3 \approx 5 \cdot 10^5$ V, and the current circulating between Io and Jupiter as measured by Voyager $\approx$ a few 10^6 A - see Acuña et al., [1981]). A last important feature is that the brightness of the IR spot appears anticorrelated to the Jovian decameter emission [Connerney et al., 1993].

Several of these results obtained in the Radio, IR and UV ranges, can be organized into a qualitatively coherent picture according to the following scenario: Io's motion through the Jovian magnetic field excites Alfvèn waves, which in turn accelerate electrons to a few keV (or more) towards the planet. When a precipitating electron population reaches the planet in a weak field region, its mirror point is very low and heavy collisional losses are sustained in the upper atmosphere, heating it and producing IR radiation but little or no radio (decameter) emission due to the tenuous reflected population. Conversely, arriving in a strong field region, the electron population is mostly reflected back, except for the loss-cone which makes it unstable with respect to the Cyclotron-Maser process [Wu and Lee, 1979], producing then intense radio emission but little or no IR radiation. The downgoing population, which does not possess any loss-cone feature, is less susceptible to amplify radio waves, which may explain the quasi-absence of positively drifting bursts.

However, this promising scenario does not explain the discrete, pulsed character of S-bursts, neither their ultra-fine structure (see section 5 below). Inconsistencies between lags may be attributed to yet undetected high-order multipolar terms of the magnetic field near the surface of the planet, and are thus little constraining. The unicity of the IR or UV spot is more puzzling when compared to the multiple radio arcs observed commonly.

Crary (1997) has developed an analytical model for the production of Alfvèn waves by Io and the subsequent acceleration of charged particles, which main results are also summarized in Table 1. He predicts some 10^{11} W for the total power of electronic precipitations with energies in the range $1 - 500$ keV ($< E >= 78$ keV), of which about 10^9 W goes into the keV range. This result is consistent with IR and UV figures, but it raises a major energy problem in the radio range: if S-bursts are produced only by keV electrons (as for the terrestrial kilometric radiation and presumably also for other planetary auroral radio emissions), then the comparison of the emitted radio power and of the power precipitated in the keV range implies an efficiency of $10 - 100\%$ for the microscopic wave generation mechanism, far too large for any known mechanism, including the most efficient ones involving direct conversion of the electrons' kinetic energy into wave energy ($< 1\%$ for the Cyclotron-Maser mechanism, [Le Quéau, 1988]. The solution of this "energy crisis" -still an open question- requires either a source of precipitated power much larger than the 10^{12} W produced by Io's motion across the Jovian magnetic field (like reconnection in Io's wake, [Goertz and Deift, 1973], or a mechanism of energy storage and sudden release (which might account for the discrete nature of S-bursts, like for example current filament disruptions, [Ryabov, 1994], or alternately another radioemission mechanism consuming the electrons energy in a spectrum much broader than a few keV.

5 Fine Structure

The database built through the above automated recognition algorithm counts about 10^5 S-bursts recorded with 10 msec $\times$ $\delta f \approx 13$ kHz resolutions between December 1993 and May 1994. It is well-suited to a large-scale analysis of the fine structure of S-bursts. We present below a preliminary analysis of the intensity profiles of individual bursts. When "following" a burst in the f-t plane, time and frequency intervals are related to each other through the burst drift-rate (here about -20 MHz/s), and distances along the corresponding magnetic field line are deduced via the parallel speed of the source (about $2 \cdot 10^4$ km/s).

Figure 4 displays intensity profiles for S-bursts of Figure 1 covering ≥ 2 MHz total band. Each S-burst appears to be excusively made of a series of spikes $100 - 200$ kHz wide (or equivalently lasting for $5 - 10$ msec, corresponding to $100 - 200$ km parallel extent along the field line). These spikes seem randomly distributed along the bursts, and are uncorrelated between successive bursts. Intensity goes back down to the background level between the spikes. They may be linked either to microstructures of depleted density (for example, $f_{pe}/f_{ce} \leq 10^{-2}$ is required for efficient Cyclotron- Maser instability, [Hilgers and de Feraudy, 1992], as suggested by Carr et al., [this volume], or more plausibly to short-lived small-scale acceleration regions (with intense parallel electric field - Alfvèn waves for example).

Figure 5 displays a "composite" integrated profile, obtained after integration over a few tens of S-bursts. The left part (solid line) is obtained by summing the intensity profiles

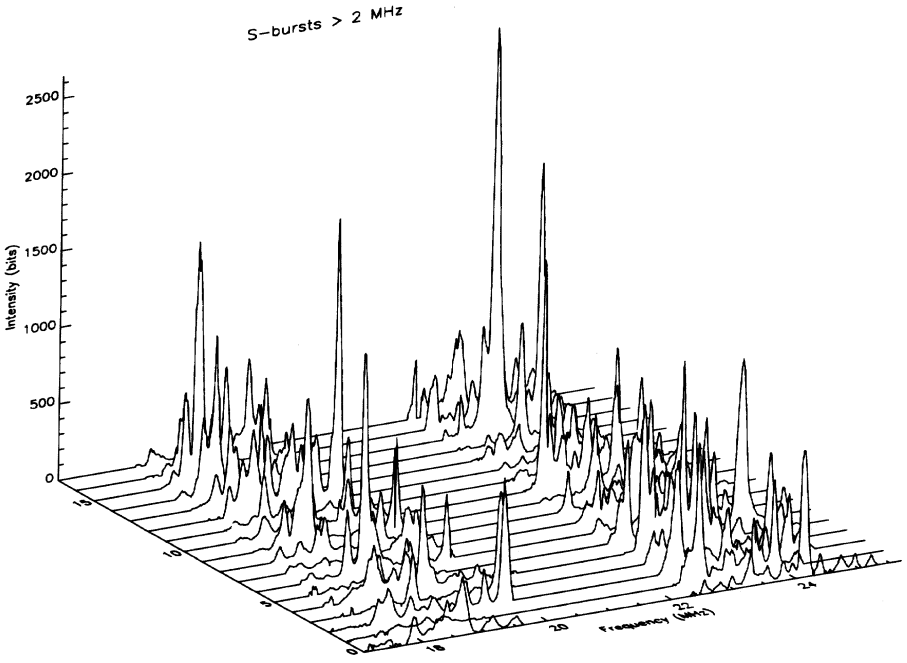

Figure 4: Intensity profiles of S-bursts of Figure 1 covering ≥ 2 MHz total band. They are entirely made of randomly distributed, uncorrelated spikes.

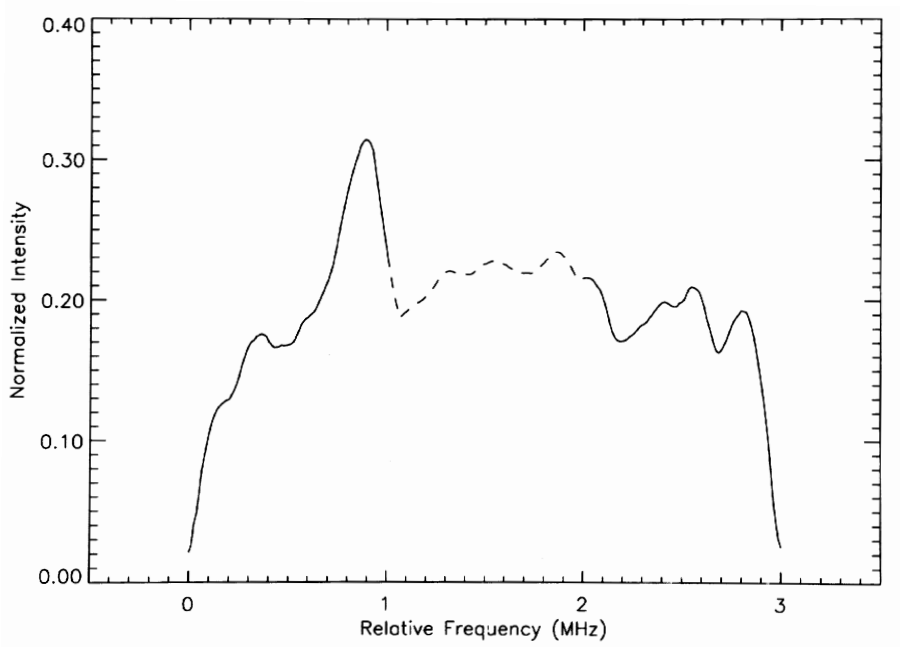

Figure 5: Integrated S-burst intensity profile, obtained after integration over the 36 bursts of Figure 4. The left part (solid line) is calculated as $\sum[I(f - f_{min})/I_{max}(f - f_{min})]$*, and the right part as* $\sum[I(f - f_{max} + 3)/I_{max}(f - f_{max} + 3)]$*, with frequencies in MHz. The middle part (dashed) is actually of variable width for each burst, due to their different total bandwidths.*

of the bursts of Figure 4 - normalized to their maximum intensity, in order to give each S-burst the same statistical weight - after aligning them to the same minimum frequency (arbitrary set to 0 MHz on the plot). The right part (solid line) is obtained in the same way, but aligning S-bursts to the same maximum frequency (set here to 3 MHz). The middle part (dashed) is actually of variable width for each burst because they have different total bandwidths. For any few tens or hundreds of S-bursts, the resulting profile integrated that way displays the characteristic shape of Figure 5, i.e. smooth and approximately flat (the local maximum at 0.9 MHz is simply due to a particularly intense spike in one of the 36 S-bursts integrated to build this profile), with steep decreases down to zero intensity on both edges, in $\sim$ 200 kHz. As 200 kHz represent $\geq$ 15 pixels in the spectrograph used, these features are highly significant. The same result is obtained separately for each of the two bands of Figure 1, i.e. $\sim 17 - 21$ MHz and $22 - 25$ MHz.

A similar behaviour is observed in the time domain for the superfine structure of pulsar radio pulses: individual pulses show a great diversity, while the average pulse profile (over a few hundred pulses) is very stable (see for example Manchester, [1977]). Although there is no definitive explanation for this superfine structure, it is qualitatively interpreted as the signature of small-scale radiating regions, while the stable integrated pulse profile carries information on the large scale geometry of the source region in the pulsar magnetosphere. By analogy, while the S-bursts fine structure is attributed to small-scale and short-lived density and/or acceleration structures, the average profile of Figure 5 can be well explained by the combination of the magnetic field topology near the IFT and the sharp emission beaming: a $\sim$ 3 MHz band with $\sim$ 200 kHz edges is consistent with emission beaming in a widely open ($70° - 80°$) hollow cone of $\sim 2°$ thickness, decreasing to zero on both (inner

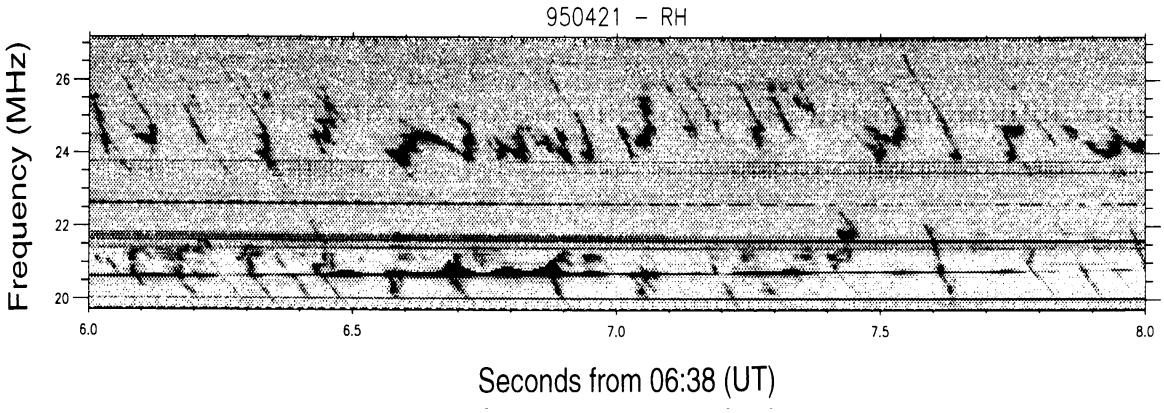

Figure 6: 2-second sample of observations with time resolution of 3.1 msec/spectrum, performed in Nançay on 1995/04/21 in right-hand circular polarization, revealing a very intricate S-bursts morphology in the f-t plane, splitted in two bands like in Figure 1.

and outer) edges in $\sim 0.2°$. Jovian emissions, and especially S-bursts, are known to be strongly beamed [Zarka, 1988], and the magnetic field topology near the planetary surface (at say, $\leq 0.5R_J$ altitude) is twisted by the presence of high-order terms [Connerney, 1992; Connerney et al., 1996]; models including 4^{th} order terms are under study). In addition, the intense currents circulating between Io and Jupiter contribute to a azimuthal component of the magnetic field, so that the field lines near the IFT could be slightly helicoidal [Ryabov, 1994], which could explain features like the favoured occurrence of S-bursts in specific frequency bands (see Ryabov et al., [this volume]), and the similar integrated profiles in each band. These effects are presently under quantitative study.

Another possibility is to attribute the shape of the integrated S-bursts intensity profile to the medium-scale (a few thousand kilometers) distribution along the field line of parameters like f_{pe}/f_{ce} which allow or not the resonance between electrons and waves to occur. The $\sim$ 200 kHz edges would correspond in that case to the sharp transition between resonance and non-resonance (see for example Galopeau et al., [1989]).

6 Perspectives

With the new observations and analyses available, the study of S-bursts is full of perspectives:

- **Observations** with 3.1 msec/spectrum resolution are performed in Nançay since 1995 (Figure 6). They reveal a very intricate S-bursts morphology in the f-t plane (see also Ryabov et al., [this volume]). Beginning in winter 1996-97, S-bursts observations will be performed simultaneously in right-hand and left-hand circular polarization in Nançay (they were performed mostly in right-hand polarization only, up to now), which will give important constraints to the emission mechanism. Multispectral observations (simultaneously in the Radio, UV and IR ranges) have proven very useful, especially for the energy budget in the IFT, and should be planned again in the future.

- **Analyses** of the above new observations should allow to study in details the S-bursts characteristics (drift-rates, fine structures), and hence the magnetic field topology and electrons energy and distribution, on a storm-by-storm basis, versus time and Io's longitude. In particular, more attention will be given to Io-A source, much less studied than the Io-B source and whose S-bursts morphology is often different.

- **Modelling** of the perturbed magnetic field near the IFT (due to intense field-aligned currents, and including a description of the internal planetary field up to the 4^{th} order) may allow to reproduce (at least part of) the fine f-t structure of the emission. Current filaments disruptions and electrons acceleration are also being modelled as an alternative to Alfvèn waves. A good criterion for the relevance of proposed acceleration and/or emission mechanisms is their ability to account for the quasi-periodic occurrence of S-bursts in "trains", presently not explained. Once reached, a successful model should allow to perform radio (or better, multispectral) remote sensing of IFT electrons dynamics and of the near-planet magnetic field topology.

Narrowband drifting structures not unlike Jupiter's S-bursts exist in the other planetary radio emissions as well as in some solar and stellar radio flares ([Abada-Simon, 1996]; see also Shepherd et al., [this volume], on the Earth's auroral roar fine structure). Their exact nature at Saturn, Uranus and Neptune is difficult to determine due to the 6-sec time resolution of Voyager's radio experiment., but the statistical properties of Neptunian and Jovian S-bursts appear similar at this time resolution [Zarka et al., in preparation]. Their generation raises the question of Io's equivalent in these magnetospheres as an electron acceleration source. As outlined above, some results concerning the S-bursts fine structure may be applicable to the yet poorly understood pulsar radioemissions.

Acknowledgements: The authors thank Dieter F. Vogl for his help to put this paper in final shape.